



Adsorption of C.I. Reactive Red 2 by ZnAl-layered double hydroxides: kinetics, equilibrium, and thermodynamics

Jui-Chan Huang^a, Chao-Yin Kuo^b, Chung-Hsin Wu^{c,*}, Yong-Huei Lin^c

^aYango College, Fuzhou 350015, China, Tel. 886-933343088; email: wish0718@outlook.com

^bDepartment of Environmental and Safety Engineering, National Yunlin University of Science and Technology, Yunlin, Taiwan, Tel. 886-5-5347311; email: kuocyr@ms35.hinet.net

^cDepartment of Chemical and Materials Engineering, National Kaohsiung University of Applied Sciences, 415 Chien Kung Road, Kaohsiung, Taiwan, Tel. 886-7-3814526; Fax: 886-7-3830674; email: wuch@kuas.edu.tw (C.-H. Wu), Tel. 886-970353133; email: opil123456@gmail.com (Y.-H. Lin)

Received 2 October 2016; Accepted 14 January 2017

ABSTRACT

In this investigation, the co-precipitation method is utilized to form ZnAl-layered double hydroxides (LDHs). Samples with Zn/Al ratios of 1, 2, and 3 are denoted as ZnAl1, ZnAl2, and ZnAl3, respectively, and were used as adsorbents to decolorize C.I. Reactive Red 2 (RR2). The surface characteristics of ZnAl-LDHs were measured by X-ray diffraction, specific surface area analysis, and scanning electron microscopy. The effects of RR2 concentration, ZnAl3 dose, and pH on RR2 adsorption were elucidated. Kinetic analyses were performed using pseudo-first-order and pseudo-second-order, and the intra-particle diffusion models. Equilibrium results were plotted using Langmuir, Freundlich, and Temkin isotherms. The particle size, specific surface area, pore volume, and pore width of ZnAl3 were 17 nm, 29.5 m²/g, 0.23 cm³/g, and 31 nm, respectively. The regression results revealed that the adsorption kinetics were more accurately represented by a pseudo-second-order model, and the equilibrium results were most accurately fitted using the Temkin isotherm. The maximum RR2 adsorption capacity of ZnAl3 was 66.7 mg/g. RR2 removal proceeded via physisorption, and the process parameters, enthalpy (ΔH°) and entropy (ΔS°), for ZnAl3 were determined to be -5.26 kJ/mol and 102 J/mol/K, respectively.

Keywords: Adsorption; Layered double hydroxides; Isotherm; Kinetics; Thermodynamics

1. Introduction

Dyes are significant water pollutants and are typically present in effluent from textile, leather, paper, and dye manufacturers. Discharging dyes into the hydrosphere frequently results in environmental damage as dyes give water an undesirable color and reduce the penetration of sunlight. To minimize the risk of pollution by such effluent, the effluent must be treated before it is discharged into the environment. Reactive dye production is characterized by great losses that are caused by the high solubility of the dyes, which also generate economical and environmental problems. C.I. Reactive

Red 2 (RR2), an azo dye with the most commonly used anchor – the dichlorotriazine group – was used as the parent compound in this study.

Adsorption has been found to outperform other methods for treating wastewater: it is low cost, highly efficient, simple, easy to perform, and insensitive to toxic substances. Several adsorbents, such as metal hydroxide sludge [1], chitosan [2,3], zeolite [4], carbon nanotubes (CNTs) [5], fly ash [6], wood-shaving bottom ash [7], sepiolite [8], chitin [9,10], MgAl-layered double hydroxides (LDHs) [11], and In₂TiO₅ [12], have been tested for their capacity to remove reactive dyes from wastewater, and adsorption by each adsorbent has been demonstrated to be efficient.

* Corresponding author.

The general formula of LDHs is $[M(II)_{1-x}M(III)_x(OH)_2]^{x+}(A^{n-})_{x/n} \cdot nH_2O$, where M(II) is a divalent metal cation; M(III) is a trivalent metal cation; and A^{n-} is the interlayer anion. LDHs are a family of synthetic anionic clays [13]. The hydrotalcite-type LDHs comprise positively charged hydroxide layers, which are separated by anions and water molecules, of which the interlayer anions can be exchanged. The anions in the interlayers of LDHs can be exchanged with other anions by an ion-exchange mechanism [14]; therefore, LDHs are suitable for use as adsorbents to remove anionic pollutants from wastewater. Zhang et al. [14] used ZnAl-LDHs to take up and degrade Orange II. Zhang et al. [15] coated Zn-LDHs (FeZn-, CoZn-, or AlZn-LDHs) on the surface of the natural bio-ceramic and compared its phosphorus removal efficiency with these Zn-LDHs. Their experimental results revealed that AlZn-LDHs had the highest total phosphorus removal efficiency among these Zn-LDHs. Zhou et al. [11] found that the maximum adsorption capacity of Reactive Orange 5 by MgAl-LDHs was 53.8 mg/g. No literature has addressed the adsorption efficiency of reactive dye by ZnAl-LDHs; therefore, in this study ZnAl-LDHs were used as adsorbents to decolorize RR2.

An understanding of adsorption kinetics, equilibrium, and thermodynamics is critical in supplying the basic information that is required for the design and operation of adsorption equipment. The adsorption rates were determined quantitatively, and those obtained using the pseudo-first-order and pseudo-second-order, and the intraparticle diffusion model were compared. The Langmuir, Freundlich, and Temkin isotherms were fitted to the equilibrium data. The objectives of this study were: (i) to evaluate the effects of the Zn/Al ratio on the removal of RR2 during the preparation of ZnAl-LDHs; (ii) to determine the effects of RR2 concentration, adsorbent dosage, and pH on the adsorption of RR2; (iii) to assess adsorption rates using various kinetic models; (iv) to measure the coefficients of the Langmuir, Freundlich, and Temkin isotherms, and (v) to derive changes in thermodynamic parameters – free energy (ΔG°), enthalpy (ΔH°), and entropy (ΔS°) during adsorption.

2. Materials and methods

2.1. Materials

Zinc nitrate ($Zn(NO_3)_2 \cdot 6H_2O$) and alumina nitrate ($Al(NO_3)_3 \cdot 9H_2O$) were used as precursors in the formation of Zn and Al, respectively, to generate AlZn-LDHs (Merck, USA). The RR2 ($C_{19}H_{10}Cl_2N_6Na_2O_7S_2$) was purchased from Sigma Aldrich (USA). The solution pH was controlled by adding HNO_3 or $NaOH$ during the reaction, and both reagents were purchased from Merck (USA). All chemicals were used without further purification.

2.2. Preparation of ZnAl-LDHs

ZnAl-LDHs was prepared by the co-precipitation method at pH 10. To form solution A, 80 mL of $Zn(NO_3)_2 \cdot 6H_2O$ (0.25, 0.5 or 0.75 M) and 80 mL $Al(NO_3)_3 \cdot 9H_2O$ (0.25 M) were mixed. Then, 80 mL $NaCl$ (0.2 M) was added dropwise to solution A. Finally, the mixture was adjusted to pH 10 by adding $NaOH$ (5 M) under vigorous stirring (600 rpm) for 2 h. The resultant

slurries were sealed in a Teflon-lined stainless steel autoclave and heated at 353 K for 24 h. The precipitates were collected by filtration and washed with 200 mL deionized water three times to remove any residual ions. The samples were finally dried in air at 333 K for 12 h. Samples with Zn/Al ratios of 1, 2 and 3 denoted as ZnAl1, ZnAl2 and ZnAl3, respectively.

2.3. Characterization of the adsorbents

The crystalline structure of the ZnAl-LDHs was analyzed by X-ray diffraction (XRD; Bruker D8 SSS, Germany). The accelerating voltage and applied current were 40 kV and 30 mA, respectively. The XRD patterns were recorded with 2θ values of 5° – 70° . The ZnAl-LDHs were examined by scanning electron microscopy (SEM) to determine their size and morphology (JEOL JSM-6500F, Japan), and their specific surface areas were determined by BET method using a surface area analyzer (ASAP 2010; Micromeritics, USA).

2.4. Adsorption experiments

All adsorption experiments were performed in a closed, pyramidal, glass bottle with a volume of 250 mL. Adsorption kinetics were measured over 2 h. An initial pH of 3.0 was used in all RR2 adsorption experiments, except for the experiments with variable pH in which the effect of pH on RR2 removal was studied. In adsorption experiments, 0.1 g of adsorbent was placed in a bottle that contained 200 mL of an RR2 solution with a concentration of 20 mg/L and shaken at 100 rpm. The effect of RR2 concentration on removal by ZnAl3 was investigated using [RR2] values of 20 and 40 mg/L with $[ZnAl3] = 0.5$ g/L. The effect of adsorbent concentration on removal by ZnAl3 was examined using $[ZnAl3]$ values of 0.3 and 0.5 g/L at $[RR2] = 20$ mg/L. The effect of pH on removal by ZnAl3 was studied using initial pH values of 3 and 9 at $[RR2] = 20$ mg/L and $[ZnAl3] = 0.5$ g/L. To obtain the equilibrium and thermodynamic parameters, adsorption experiments were conducted at 298, 318, and 328 K over 24 h. Suspended particles were separated by filtering through a 0.22- μ m filter (Millipore). The RR2 concentration was measured using a spectrophotometer (Hitachi U-2001) at 538 nm. Decolorization efficiency was obtained from the difference between RR2 concentrations before and after experiments. Most experiments were performed in duplicate, and values shown are averages.

3. Results and discussion

3.1. Surface characteristics of ZnAl-LDHs

Fig. 1 shows the XRD patterns of ZnAl-LDHs. The diffraction peaks of all of the ZnAl-LDHs at 2θ equal to 11.7° , 23.4° , 34.6° , 39.2° , and 46.7° are assigned to the (0 0 3), (0 0 6), (0 1 2), (0 1 5) and (0 1 8) crystal faces of standard LDHs, respectively. The peaks of ZnAl1, ZnAl2, and ZnAl3 barely change with the Zn/Al ratio of ZnAl-LDHs (JCPDS (Joint Committee on Powder Diffraction Standards) No. 38-0486). Accordingly, all of the samples have the typical LDHs structure. Moreover, the intensity of (0 0 3) crystal face showed the order ZnAl3 > ZnAl2 > ZnAl1. The diffraction peaks of ZnAl2 and ZnAl3 at 2θ equal to 31.8° , 36.3° , 56.6° and 62.9°

are assigned to the (1 1 0), (1 1 3), (3 0 0) and (1 1 9) crystal faces of standard $\text{Zn}(\text{OH})_2$, respectively (JCPDS No. 48-1066). The intensity of the XRD peaks of $\text{Zn}(\text{OH})_2$ increased with the $\text{Zn}^{2+}/\text{Al}^{3+}$ ratio. Using the Scherrer equation, the particle sizes of ZnAl1, ZnAl2, and ZnAl3 were calculated to be 11, 15, and 17 nm, respectively. The specific surface areas of ZnAl1, ZnAl2, and ZnAl3 were 56.9, 18.5, and 29.5 m^2/g , respectively; the pore widths were 11, 24, and 31 nm, and the pore volumes were 0.15, 0.11, and 0.23 cm^3/g , respectively.

SEM was utilized to characterize the surface structure and morphology of ZnAl-LDHs and to determine their shape and pore structures in particular. The surface of ZnAl-LDHs comprised overlapping crystals in the form of stacked layers (Fig. 2). Wen et al. [13] found that ZnAl-LDHs have a hexagonal layered structure, which is typical of hydrotalcite-like material. ZnAl samples exhibited the typical plate-like morphology of LDHs with a lamellar structure.

3.2. Effects of Zn/Al ratio, RR2 concentration, adsorbent dose, and pH on RR2 removal

Fig. 3 plots the effects of Zn/Al ratio in the preparation of ZnAl-LDHs on RR2 removal. After the reaction had proceeded for 30 min, the percentages of RR2 adsorbed onto ZnAl1, ZnAl2, and ZnAl3 were 65%, 76%, and 85%, respectively. The adsorption process was rapid for the first 60 min, after which time its rate gradually decreased

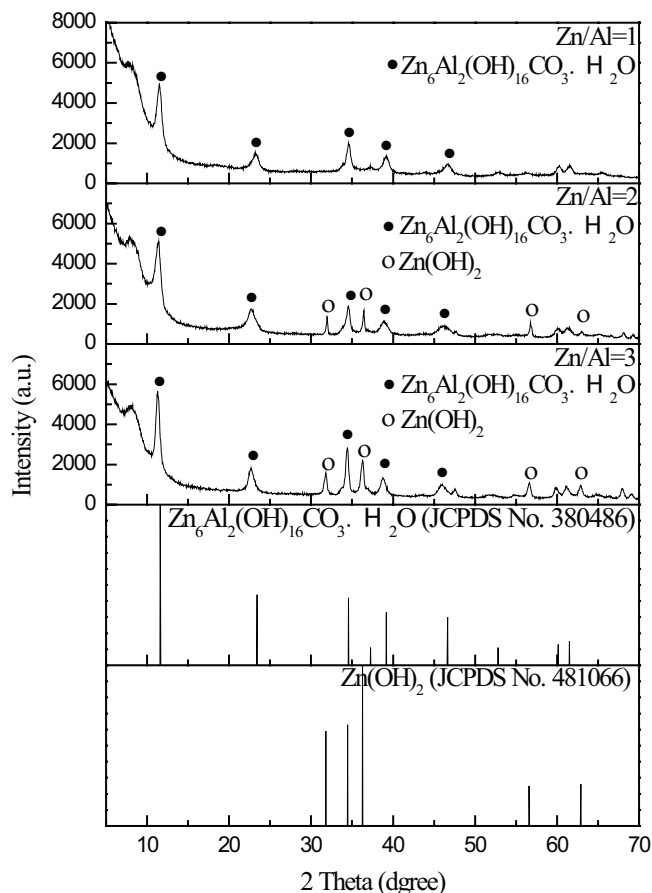


Fig. 1. XRD patterns of ZnAl-LDHs.

until equilibrium was reached. Initially, all surface sites on the adsorbent were vacant, and the RR2 concentration gradient was relatively high, so the initial adsorption rate was high. This initial phase may be explained by passive uptake via physical adsorption or ion exchange at the surface [16]. In this investigation, the molar ratio of Zn^{2+} to

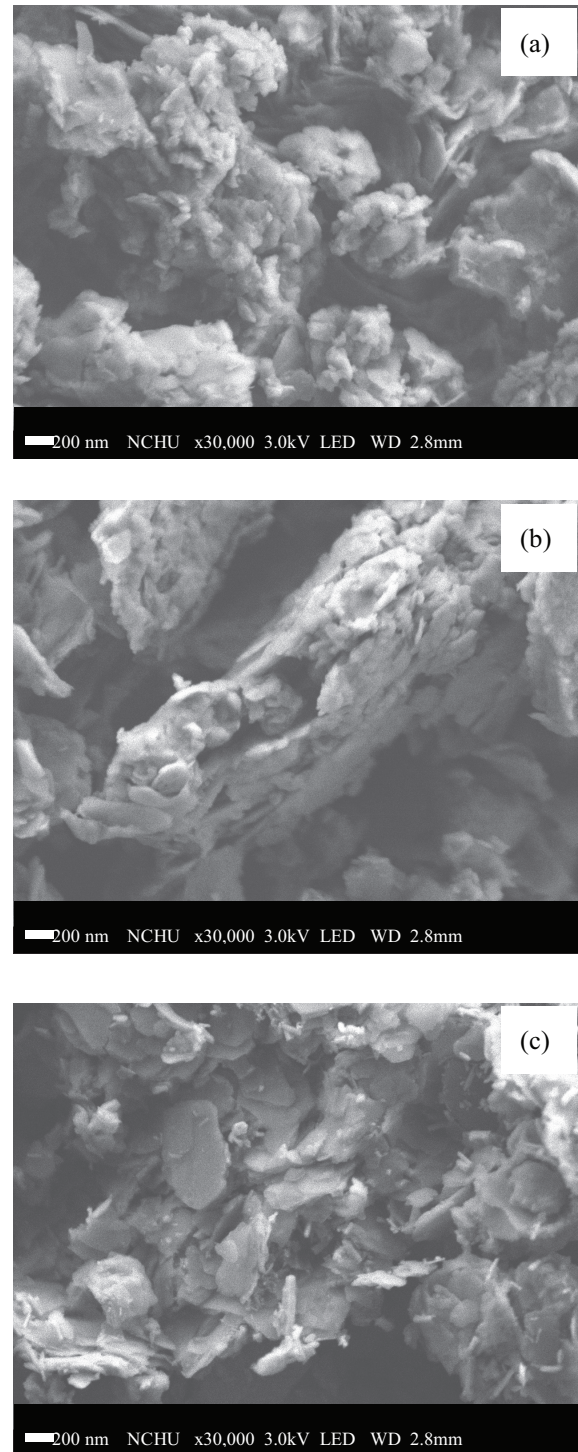


Fig. 2. SEM micrographs of ZnAl-LDHs: (a) ZnAl1, (b) ZnAl2, and (c) ZnAl3.

Al³⁺ was in the range 1:1–3:1. The Zn/Al ratio can be used to tune the layer charge density, the inherent ion exchange capacity, and the interlamellar anion concentration in ZnAl-LDHs [14]. The experimental results herein suggested that increasing the initial amount of Zn²⁺ ions increases the size of ZnAl-LDHs crystals (from 11 to 17 nm). In XRD analysis (Fig. 1), ZnAl3 had the (0 0 3) crystal face that yielded the most intense signal, and the largest mean crystal size, suggesting that it most strongly adsorbed RR2. Of the samples, ZnAl3 exhibited the highest adsorption efficiency for RR2, so ZnAl3 was used as the model adsorbent to analyze kinetics, equilibrium, and thermodynamics.

The anions of RR2 intercalate in the interlayer of ZnAl-LDHs with SO₃ groups that are bonded to metal ions and hydroxyl groups in two layers of LDHs via electrostatic attraction and hydrogen bonding, respectively. ZnAl-LDHs adsorb ionic molecules in the solution by surface adsorption and ionic exchange, depending on the charge-balancing anions in the interlayer, and the charge density of the ZnAl-LDHs [14]. This study uses XRD findings and adsorption results to propose mechanisms by which ZnAl3 adsorbs RR2. Eqs. (1)–(4) describe the formation of ZnAl3. Eq. (5) describes the surface adsorption of RR2 on ZnAl3, and Eq. (6) describes the ionic exchange process of RR2 on ZnAl3.

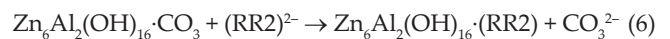
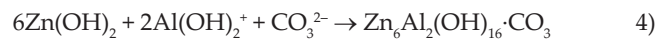


Fig. 4 plots the effects of adsorbent dose, RR2 concentration, and pH on the adsorption of RR2 by ZnAl3. Increasing the ZnAl3 dosage increased RR2 adsorption, mainly because of the increase in adsorptive surface area and availability of adsorption sites on ZnAl3. However, the amount of RR2 adsorbed per unit mass of ZnAl3 declined as the ZnAl3 dose increased (Table 1). The decrease in unit adsorption as the ZnAl3 dose increased follows from the fact that adsorption sites remain unsaturated during the adsorption process, and possibly from the fact that adsorption sites overlap because of ZnAl3 particle overcrowding. Several studies have also determined that unit adsorption capacity declines as the adsorbent dosage increases [17,18].

The RR2 removal percentage declined as the initial RR2 concentration increased, even though the amount of RR2 adsorbed per unit mass of ZnAl3 increased with the initial RR2 concentration (Table 1). This increase is caused by an increase in the driving force of the concentration gradient as the initial RR2 concentration increases. Various studies have found that adsorption capacity increases with the dye concentration [17–19].

Solution pH is an important adsorption parameter because pH depends on complex reactions or electrostatic interactions in physisorption processes at the adsorption surface. Reducing pH increased the adsorption of RR2 onto ZnAl3. At a lower solution pH, more H⁺ causes more hydroxyl groups to become protonated (–OH₂⁺) on the surface of ZnAl3, promoting the electrostatic attraction between the surface of ZnAl3 and the –SO₃[–] group in RR2. At a higher solution pH, the surfaces of ZnAl3 are more negatively charged, causing a stronger electrostatic repulsion between negatively charged surface sites and the –SO₃[–] groups of RR2.

The adsorption kinetics of an adsorbent determines the rate of the adsorption process. The pseudo-first-order model [20], pseudo-second-order model [20,21], and intraparticle diffusion model [22] were used to fit the experimental data and determine the adsorption kinetics. Eq. (7) is the pseudo-first-order model:

$$\ln(q_e - q) = \ln(q_e) - k_1 t \quad (7)$$

where q_e and q (mg/g) are the amounts of RR2 that are adsorbed on the adsorbent at equilibrium and at time t , respectively,

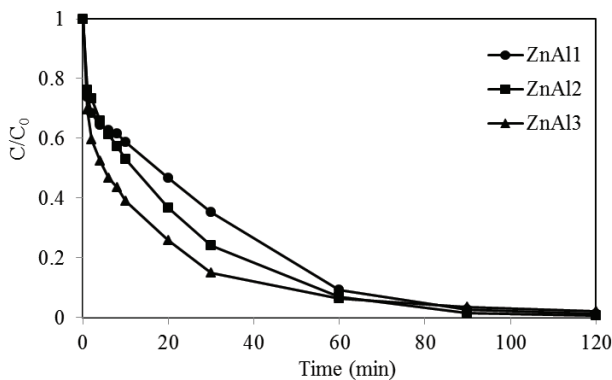


Fig. 3. Effect of Zn/Al ratio in preparation of ZnAl-LDHs on RR2 adsorption ([RR2] = 20 mg/L, [adsorbent] = 0.5 g/L, pH = 3, and T = 298 K).

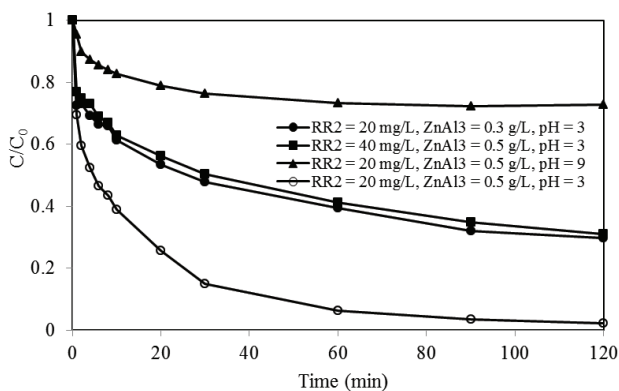


Fig. 4. Effects of adsorbent dose, RR2 concentration and pH on adsorption of RR2 by ZnAl3.

Table 1
Kinetic parameters of RR2 removal by ZnAl-LDHs

Pseudo-first-order model	$q_{e,exp.}$ (mg/g)	k_1 (min ⁻¹)	$q_{1e,cal.}$ (mg/g)	R^2
[RR2] = 20 mg/L, [ZnAl1] = 0.5 g/L, pH 3	36.3	0.0237	29.3	0.990
[RR2] = 20 mg/L, [ZnAl2] = 0.5 g/L, pH 3	37.2	0.0389	31.3	0.999
[RR2] = 20 mg/L, [ZnAl3] = 0.5 g/L, pH 3	37.5	0.0495	26.4	0.990
[RR2] = 20 mg/L, [ZnAl3] = 0.3 g/L, pH 3	40.3	0.015	49.0	0.984
[RR2] = 40 mg/L, [ZnAl3] = 0.5 g/L, pH 3	47.1	0.015	60.8	0.975
[RR2] = 20 mg/L, [ZnAl3] = 0.5 g/L, pH 9	10.6	0.007	36.2	0.836
Pseudo-second-order model	$q_{2e,cal.}$ (mg/g)	k_2 (g/mg/min)	R^2	
[RR2] = 20 mg/L, [ZnAl1] = 0.5 g/L, pH 3	27.4	0.0088	0.960	
[RR2] = 20 mg/L, [ZnAl2] = 0.5 g/L, pH 3	34.1	0.0050	0.959	
[RR2] = 20 mg/L, [ZnAl3] = 0.5 g/L, pH 3	36.6	0.0075	0.985	
[RR2] = 20 mg/L, [ZnAl3] = 0.3 g/L, pH 3	36.9	0.0086	0.981	
[RR2] = 40 mg/L, [ZnAl3] = 0.5 g/L, pH 3	42.4	0.0070	0.983	
[RR2] = 20 mg/L, [ZnAl3] = 0.5 g/L, pH 9	10.7	0.0020	0.995	
Intraparticle diffusion model	k_i (mg/g/min ^{0.5})	C (mg/g)	R^2	
[RR2] = 20 mg/L, [ZnAl1] = 0.5 g/L, pH 3	3.231	7.198	0.977	
[RR2] = 20 mg/L, [ZnAl2] = 0.5 g/L, pH 3	4.710	4.176	0.997	
[RR2] = 20 mg/L, [ZnAl3] = 0.5 g/L, pH 3	4.636	9.211	0.987	
[RR2] = 20 mg/L, [ZnAl3] = 0.3 g/L, pH 3	3.952	12.91	0.981	
[RR2] = 40 mg/L, [ZnAl3] = 0.5 g/L, pH 3	4.884	13.10	0.991	
[RR2] = 20 mg/L, [ZnAl3] = 0.5 g/L, pH 9	1.544	1.590	0.932	

and k_1 (min⁻¹) is the rate constant of the pseudo-first-order model. Eq. (8) is the pseudo-second-order model:

$$\frac{t}{q} = \frac{1}{k_2 q_e^2} + \frac{t}{q_e} \quad (8)$$

where q_e and q (mg/g) are as defined for the pseudo-first-order model, and k_2 (g/mg·min) is the rate constant of the pseudo-second-order model. Since neither model yielded a potential diffusion mechanism, kinetic results were analyzed using the intraparticle diffusion model. In the intraparticle diffusion model, film diffusion was negligible, and intraparticle diffusion was the only rate-controlling step. Eq. (9) is the intraparticle diffusion model:

$$q = k_i t^{1/2} + C \quad (9)$$

where C (mg/g) is the intercept value, and k_i (mg/g·min^{0.5}) is the intraparticle diffusion rate constant.

Table 1 presents the kinetic parameters of RR2 removal by ZnAl-LDHs. The q values ($q_{e,cal.}$) that were calculated using the pseudo-second-order model were more consistent with the experimental q values ($q_{e,exp.}$) than those calculated using the pseudo-first-order model. Therefore, this study suggests that the pseudo-second-order model more accurately represents the adsorption kinetics. A similar result has been obtained concerning the adsorption of RR2 by chitin [10], CNTs [5], and In₂TiO₅ [12]. When the regression of q as a function of $t^{1/2}$ is linear and passes through the origin, intraparticle diffusion is the only rate-limiting step [19].

Although the regression was linear, the plot did not pass through the origin (Table 1), suggesting that adsorption involved intraparticle diffusion, but that it was not the only rate-controlling step. Other kinetic mechanisms probably controlled the adsorption rate, which finding is consistent with one obtained by other adsorption studies [5,10]. Akkaya et al. [9] suggested that pore diffusion and surface diffusion occur simultaneously within the adsorbent particle. RR2 adsorption capacities ($q_{2e,cal.}$) followed the order ZnAl3 > ZnAl2 > ZnAl1. This experimental result reveals that ZnAl3 had the highest density of active sites. The adsorption rates (k_2) followed the order ZnAl1 > ZnAl3 > ZnAl2, as did the surface areas of ZnAl-LDHs. Accordingly, increasing the surface area shortened the equilibrium time of RR2 adsorption.

3.3. Adsorption isotherms

The adsorption isotherm is the most important information, which explicates how adsorbate molecules are distributed between the liquid phase and solid phase when the adsorption process is at equilibrium. The equation parameters and thermodynamic assumptions that underlie these equilibrium isotherms commonly provide insights into the adsorption mechanisms, surface properties, and affinities of the adsorbent. Langmuir [23], Freundlich [24], and Temkin [25] isotherms were used herein to describe the observed adsorption equilibrium. The Langmuir isotherm assumes monolayer coverage of the adsorption surface and no subsequent interaction among adsorbed molecules. Therefore, the adsorption saturates, and then no further adsorption can occur. Eq. (10) describes the Langmuir isotherm:

$$q_e = \frac{q_m K_L C_e}{(1 + K_L C_e)} \tag{10}$$

where q_e is the mass of RR2 that is adsorbed per unit mass of ZnAl3 (mg/g) at equilibrium; C_e is the aqueous concentration of RR2 (mg/L) at equilibrium; K_L is the Langmuir constant (L/mg) that is related to the affinity of binding sites; and q_m is the maximum adsorption capacity (mg/g). Parameters q_m and K_L are obtained from the intercept and slope of the best linear fit of $1/q_e$ as a function of $1/C_e$.

The Freundlich isotherm is an empirical relationship that describes multilayer adsorption on heterogeneous surface sites, and is given by Eq. (11):

$$q_e = K_F C_e^{1/n} \tag{11}$$

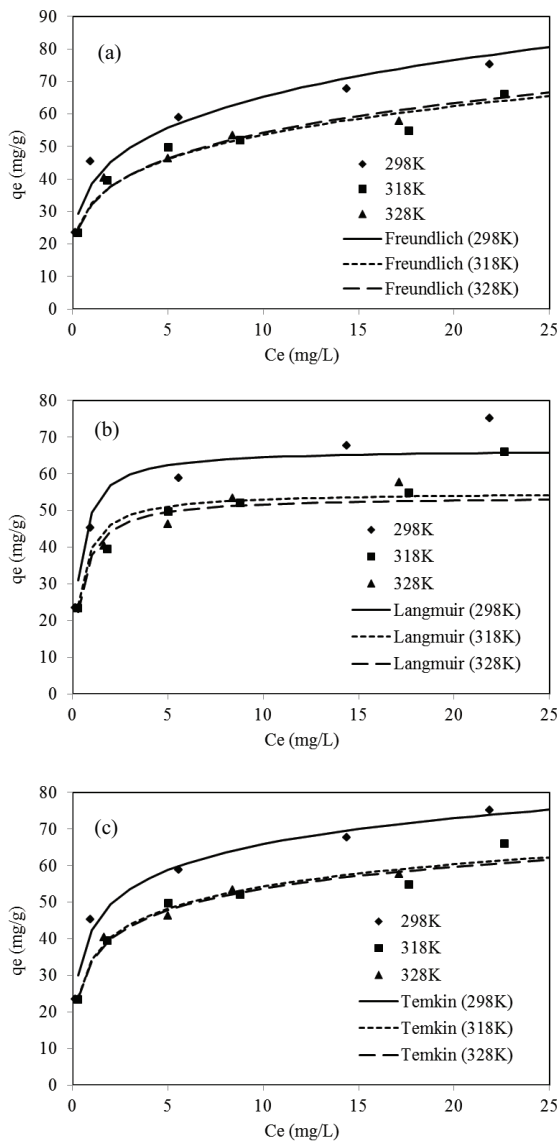


Fig. 5. Isotherms for the adsorption of RR2 on ZnAl3 at various temperatures: (a) Freundlich, (b) Langmuir, and (c) Temkin.

where q_e and C_e are as defined as above, and K_F and n are Freundlich constants that specify the adsorption capacity and adsorption strength, respectively. Parameters K_F and $1/n$ are obtained from the intercept and slope of the best linear fit of $\ln(q_e)$ as a function of $\ln(C_e)$.

The Temkin model assumes that the heat of adsorption of all molecules in a layer declines linearly as surface coverage increases owing to adsorbent–adsorbate interactions. Adsorption is characterized by a uniform distribution of binding energies up to a maximum value. The Temkin isotherm describes the behavior of adsorption systems on a heterogeneous surface. Eq. (12) gives the linear form of the Temkin isotherm:

$$q_e = B_1 \ln(K_i) + B_1 \ln(C_e) \tag{12}$$

where B_1 is a constant that is related to heat of adsorption, and K_i is the equilibrium binding constant (L/mol) that corresponds to the maximum binding energy. A plot of q_e as a function of $\ln(C_e)$ yields constants of the isotherm.

Fig. 5 displays different isotherms at various temperatures for the adsorption of RR2 on ZnAl3. The adsorption capacities increased with concentration, up to a plateau, which represents the maximum adsorption capacity. Table 2 presents the isotherm parameters for the RR2 removal by ZnAl3. The high correlation coefficient of the Temkin isotherm reveals that it accurately describes the adsorption process, suggesting that the adsorption system was on a heterogeneous surface. In most cases, an exponent between $1 < n < 10$ indicates beneficial adsorption [3]. The value of $1/n$ in the Freundlich model is significantly less than one in this study, revealing a favorable adsorption system. If n is below unity, then the adsorption is chemical; otherwise, the adsorption is physical [26]. All values of n exceeded 4, suggesting that the adsorption of RR2 on ZnAl3 is physical. Notably, K_L , q_m , K_F , and B_1 declined as the temperature increased, suggesting that RR2 adsorption on ZnAl3 increased as the temperature declined (Table 2).

3.4. Thermodynamic analyses

Thermodynamic parameters provide in-depth information concerning the energetic changes that are associated

Table 2
Isotherm parameters of RR2 removal by ZnAl3 (pH = 3)

Langmuir constants	K_L (L/mg)	q_m (mg/g)	R^2
298 K	2.88	66.7	0.986
318 K	2.60	55.0	0.955
328 K	2.36	53.8	0.981
Freundlich constants	K_F	n	R^2
298 K	38.6	4.37	0.949
318 K	32.5	4.60	0.964
328 K	32.3	4.44	0.961
Temkin constants	B_1	K_i (L/mol)	R^2
298 K	10.2	62.1	0.988
318 K	8.68	51.9	0.958
328 K	8.58	52.4	0.988

with adsorption; therefore, these parameters must be evaluated accurately. Changes to ΔG° , ΔH° , and ΔS° were calculated to elucidate the adsorption process. These values were obtained from the Langmuir isotherm and Eqs. (13) and (14):

$$\Delta G^\circ = -RT \ln(K_L) \quad (13)$$

$$\ln(K_L) = \frac{\Delta S^\circ}{R} - \frac{\Delta H^\circ}{RT} \quad (14)$$

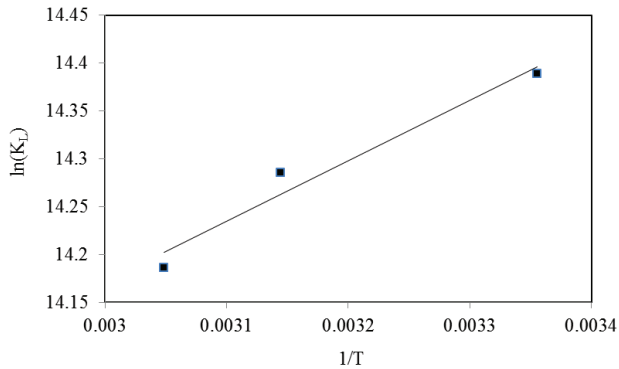


Fig. 6. Dependence of adsorption on temperature, shown as van 't Hoff plot.

Table 3
Thermodynamic parameters of RR2 adsorption onto ZnAl3

	ΔG° (kJ/mol)	ΔH° (kJ/mol)	ΔS° (J/mol·K)
298 K	-35.7	-5.26	102
318 K	-37.8		
328 K	-38.7		

where K_L is the Langmuir equilibrium constant (L/mol); R is the gas constant (8.314×10^{-3} kJ/mol·K); and T is the temperature (K). ΔH° and ΔS° were obtained from the slope and intercept of the van 't Hoff plot of $\ln(K_L)$ as a function of $1/T$ [27].

Fig. 6 shows the van 't Hoff plot. Table 3 presents the thermodynamic parameters of the RR2 adsorption onto ZnAl3. The ΔG° values were negative at all tested temperatures, confirming that the adsorption of RR2 onto ZnAl3 was spontaneous and thermodynamically favorable. The positive ΔS° values suggest an increase in the randomness at the solid–solution interface during RR2 adsorption onto ZnAl3. Physisorption and chemisorption can be identified, in part, by the magnitude of the enthalpy change. The change in adsorption enthalpy for physisorption is in the range of -20 – 40 kJ/mol [28]. The value of ΔH° suggests that the adsorption of RR2 onto ZnAl3 involved physisorption. The negative ΔH° value suggested that the adsorption of RR2 onto ZnAl3 is exothermic, which finding is supported by the drop in the adsorption of RR2 as the temperature increases. This effect may follow from the fact that an increase in temperature reduces the adsorptive forces between RR2 and the active sites on the ZnAl3 surface, reducing the adsorption.

Table 4 compares the adsorption capacities of various adsorbents for reactive dyes and the relevant thermodynamic parameters, taken from the literature. The adsorption

Table 4
Adsorption characteristics of reactive dyes in various adsorbents

Adsorbent	Dye	Adsorption capacity (mg/g)	Conditions	ΔS° (J/mol·K)	ΔH° (kJ/mol)	References
ZnAl3	RR2	66.7	298 K, pH 3	102	-5.26	This study
Chitin	RR2	20.2	298 K, pH 5	152.10	16.34	[10]
CNTs	RR2	39.8	301 K, pH 6.5	216.99	31.55	[5]
In ₂ TiO ₅	RR2	70.5	298 K, pH 3	-	-	[12]
		27.3	298 K, pH 7	-	-	
Metal hydroxide sludge	RR2	61.7	303 K, pH 8–9	-	-5.56	[1]
	RR120	45.9			2.77	
	RR141	51.6			6.41	
MgAl-LDHs	RO5	53.8	298 K, pH 6.5	151.34	38.23	[11]
Chitosan	RR141	67.9	293 K, pH 11	-37.88	-18.20	[2]
Surfactant-modified zeolite	RR239	15.9	303 K, pH 5	-14.029	-11.964	[4]
	RB5	112.9		-23.207	-6.891	
Fly ash	RB*19	135.7	293 K, pH 6	122	28.85	[6]
	RR198	47.3		63	13.93	
	RY84	37.3		64	13.29	
Wood-shaving bottom ash	RR141	30.8	293 K, pH 11	165	26.38	[7]
Turkish Sepiolite	RB*15	32.0	295 K, pH 6	15	1.95	[8]

Note: RR – Reactive Red; RO – Reactive Orange; RB – Reactive Black; RB* – Reactive Blue; and RY – Reactive Yellow.

capacity of each adsorbent for a reactive dye is determined by its properties, such as structure, functional groups, and surface area. For metal hydroxide sludge, chitosan, and surfactant-modified zeolite, the adsorption of reactive dye is an exothermic process. Furthermore, most adsorption of reactive dyes onto most of the adsorbents herein, excluding chitosan and surfactant-modified zeolite, exhibited a positive entropic change. The capacity of ZnAl₃ to adsorb RR2, an anionic dye, exceeded that of chitin and CNTs. Although the RR2 adsorption capacity of In₂TiO₅ exceeded that of ZnAl₃, so did its cost. This study suggests that the cost of ZnAl₃ is reasonable, and the adsorption capacity of ZnAl₃ is acceptable for practical wastewater treatment, so ZnAl₃ has important advantages over other adsorbents.

4. Conclusions

In this investigation, co-precipitation was used to synthesize ZnAl-LDHs as an adsorbent to remove RR2. The RR2 adsorption efficiency was highest when the Zn/Al ratio was 3. Increasing the ZnAl₃ dosage increased RR2 adsorption, whereas increasing the RR2 concentration or pH reduced RR2 adsorption. According to kinetic analyses, the adsorption involved intraparticle diffusion, but this was not the only rate-controlling step. Equilibrium isotherm analyses suggested that RR2 was adsorbed onto a heterogeneous surface. The adsorption of RR2 onto ZnAl₃ was a spontaneous, exothermic process that involved physisorption.

Acknowledgment

The authors would like to thank the National Science Council of the Republic of China, Taiwan, for financially supporting this research under Contract No. MOST 105-2221-E-151-001.

References

- [1] S. Netpradit, P. Thiravetyan, S. Towprayoon, Adsorption of three azo reactive dyes by metal hydroxide sludge: effect of temperature, pH, and electrolytes, *J. Colloid Interface Sci.*, 270 (2004) 255–261.
- [2] N. Sakayawong, P. Thiravetyan, W. Nakbanpote, Adsorption mechanism of synthetic reactive dye wastewater by chitosan, *J. Colloid Interface Sci.*, 286 (2005) 36–42.
- [3] G. Annadurai, L.Y. Ling, J.F. Lee, Adsorption of reactive dye from an aqueous solution by chitosan: isotherm, kinetic and thermodynamic analysis, *J. Hazard. Mater.*, 152 (2008) 337–346.
- [4] D. Karadag, M. Turan, E. Akgul, Adsorption equilibrium and kinetics of Reactive Black 5 and Reactive Red 239 in aqueous solution onto surfactant-modified zeolite, *J. Chem. Eng. Data*, 52 (2007) 1615–1620.
- [5] C.H. Wu, Adsorption of reactive dye onto carbon nanotubes: equilibrium, kinetics and thermodynamics, *J. Hazard. Mater.*, 144 (2007) 93–100.
- [6] N. Dizge, C. Aydinler, E. Demirbas, M. Kobya, S. Kara, Adsorption of reactive dyes from aqueous solutions by fly ash: kinetic and equilibrium studies, *J. Hazard. Mater.*, 150 (2008) 737–746.
- [7] P. Leechart, W. Nakbanpote, P. Thiravetyan, Application of 'waste' wood-shaving bottom ash for adsorption of azo reactive dye, *J. Environ. Manage.*, 90 (2009) 912–920.
- [8] A. Tabak, E. Eren, B. Afsin, B. Caglar, Determination of adsorptive properties of a Turkish Sepiolite for removal of Reactive Blue 15 anionic dye from aqueous solutions, *J. Hazard. Mater.*, 161 (2009) 1087–1094.
- [9] G. Akkaya, I. Uzun, F. Guzel, Kinetics of the adsorption of reactive dyes by chitin, *Dyes Pigm.*, 73 (2007) 168–177.
- [10] C.H. Wu, C.Y. Kuo, C.H. Yeh, M.J. Chen, Adsorption of C.I. Reactive Red 2 from aqueous solutions by chitin: an insight into kinetics, equilibrium, and thermodynamics, *Water Sci. Technol.*, 65 (2012) 490–495.
- [11] Q. Zhou, F. Chen, W. Wu, R. Bu, W. Li, F. Yang, Reactive orange 5 removal from aqueous solution using hydroxyl ammonium ionic liquids/layered double hydroxides intercalation composites, *Chem. Eng. J.*, 285 (2016) 198–206.
- [12] C.H. Wu, C.Y. Kuo, C.H. Lai, W.Y. Chung, Decolorization of C.I. Reactive Red 2 by a large specific surface area In₂TiO₅: photodegradation and adsorption, *React. Kinet. Mech. Cat.*, 111 (2014) 383–392.
- [13] X. Wen, Z. Yang, X. Xie, Z. Feng, J. Huang, The effects of element Cu on the electrochemical performances of Zinc-Aluminum-hydroxaltes in Zinc/Nickel secondary battery, *Electrochim. Acta*, 180 (2015) 451–459.
- [14] L. Zhang, Z. Xiong, L. Li, R. Burt, X.S. Zhao, Uptake and degradation of Orange II by zinc aluminum layered double oxides, *J. Colloid Interface Sci.*, 469 (2016) 224–230.
- [15] X. Zhang, L. Guo, H. Huang, Y. Jiang, M. Li, Y. Leng, Removal of phosphorus by the core-shell bio-ceramic/Zn-layered double hydroxides (LDHs) composites for municipal wastewater treatment in constructed rapid infiltration system, *Water Res.*, 96 (2016) 280–291.
- [16] X. Li, Y. Tang, X. Cao, D. Lu, F. Luo, W. Shao, Preparation and evaluation of orange peel cellulose adsorbents for effective removal of cadmium, zinc, cobalt and nickel, *Colloids Surf., A*, 317 (2008) 512–521.
- [17] V. Ponnusami, S. Vikram, S.N. Srivastava, Guava (*Psidium guajava*) leaf powder: novel adsorbent for removal of methylene blue from aqueous solutions, *J. Hazard. Mater.*, 152 (2008) 276–286.
- [18] W.T. Tsai, K.J. Hsien, H.C. Hsu, C.M. Lin, K.Y. Lin, C.H. Chiu, Utilization of ground eggshell waste as an adsorbent for the removal of dyes from aqueous solution, *Bioresour. Technol.*, 99 (2008) 1623–1629.
- [19] I.D. Mall, V.C. Srivastava, N.K. Agarwal, Removal of Orange-G and Methyl Violet dyes by adsorption onto bagasse fly ash—kinetic study and equilibrium isotherm analyses, *Dyes Pigm.*, 69 (2006) 210–223.
- [20] Y.S. Ho, G. McKay, Sorption of dye from aqueous solution by pit, *Chem. Eng. J.*, 70 (1998) 115–124.
- [21] G. Blanchard, M. Maunay, G. Martin, Removal of heavy metals from waters by means of natural zeolites, *Water Res.*, 18 (1984) 1501–1507.
- [22] W.J. Weber Jr., J.C. Morris, Kinetics of adsorption on carbon from solution, *J. Sanit. Eng. Div. ASCE*, 89 (1963) 31–60.
- [23] I. Langmuir, The constitution and fundamental properties of solids and liquids. Part I. Solids, *J. Am. Chem. Soc.*, 38 (1916) 2221–2295.
- [24] H.M.F. Freundlich, Over the adsorption in solution, *J. Phys. Chem.*, 57 (1906) 385–470.
- [25] M.I. Temkin, V. Pyzhev, Kinetics of ammonia synthesis on promoted iron catalyst, *Acta Phys. Chim. USSR*, 12 (1940) 217–222.
- [26] J.Q. Jiang, C. Cooper, S. Ouki, Comparison of modified montmorillonite adsorbents. Part I. Preparation, characterization and phenol adsorption, *Chemosphere*, 47 (2002) 711–716.
- [27] R. Han, L. Zhang, C. Song, M. Zhang, H. Zhu, L. Zhang, Characterization of modified wheat straw, kinetic and equilibrium study about copper ion and methylene blue adsorption in batch mode, *Carbohydr. Polym.*, 79 (2010) 1140–1149.
- [28] L.L. Lian, L.P. Guo, C.J. Guo, Adsorption of Congo red from aqueous solutions onto Ca-bentonite, *J. Hazard. Mater.*, 161 (2009) 126–131.